Adsorption of N_2 on a porous silica substrate studied by a quartz-crystal microbalance

Yongho Seo and Insuk Yu
Department of Physics and Condensed Matter Research Institute, Seoul National University, Seoul 151-742, Korea
(Received 17 March 1999)

We studied the adsorption isotherms of N_2 on a porous silica substrate (xerogel) using a quartz crystal microbalance technique. The oscillation frequency and amplitude of oscillation were measured at 325 K and also at different temperatures in the range 76–80 K, while the pressure of N_2 gas was varied. In contrast to adsorptions on flat surfaces, which occur mostly near the saturation vapor pressure, adsorption on the porous substrate progressed in a wide range of vapor pressures. A hysteresis between the adsorption and desorption curves, which is an indication of so-called *capillary condensation*, was observed. We found a power-law relation between the vapor pressure and the amount of gases adsorbed in the intermediate coverage regime, but the relation became deviated in the thick coverage regime. We attribute the deviation to the rough and porous nature of the silica layer. [S0163-1829(99)01648-3]

I. INTRODUCTION

The quartz crystal microbalance (QCM) has been used extensively to study adsorption phenomena on flat surfaces. For example, the adsorptions of gases on metallic substrates have been studied using QCM to investigate the wetting and prewetting transitions.[1–6] On the other hand, the Brunauer-Emmett-Teller (BET) method[7–9] has been routinely applied to study adsorption phenomena on porous materials which have large surface areas (i.e., $S>10\ \mathrm{m^2/g}$). The weakness of the BET method is its low sensitivity for samples which have small surface areas. We devised an experimental method to increase the surface area of QCM by incorporating a porous silica substrate onto the surface of the quartz crystal. This makes it possible to apply the QCM technique to gas adsorption experiments on porous substrates using the BET method.

II. THEORY

When a gas molecule is adsorbed on a solid substrate, the interaction of the molecule with the substrate is described by the sum of repulsive and attractive potentials. In many cases, the attractive potential can be described by the van der Waals interaction between a gas molecule and all the particles within the solid substrate. Generally, a 9-3 potential [e.g., $v(z)=-\alpha z^{-3}+\beta z^{-9}$] is used as a function of the distance z of the molecule from the substrate.[8] Except for adsorption on a substrate with only a few atomic layers, the short-range repulsive potential does not play a dominant role.

In multilayer adsorption, the adsorption isotherm of gas molecules on a flat adsorbent can be described by the Frenkel-Halsey-Hill (FHH) theory,[8,10]

$$k_BT\ln(p/p_0)=u_P(z(p)), \tag{1}$$

where p/p_0 is the normalized pressure of adsorbing gas relative to the saturation vapor pressure p_0, z is the thickness of the adsorbed layer, and $u_P(z)\propto -z^{-s}$ is the perturbational potential energy exerted by both the adsorbent and the adsorbed layer. The exponent s is expected to be exactly 3 because $u_P(z)$ is equivalent to the long-range part $(-\alpha z^{-3})$ in the 9-3 potential. However, varieties of experimental data that have been fitted to Eq. (1) resulted in an estimate of s in the range 2.6–2.8.[9]

In the Dzyaloshinskii-Lifshitz-Pitaevskii (DLP) theory,[11] the adsorption isotherm was modified to

$$k_BT\ln(p/p_0)=-\gamma(z)z^{-s}, \tag{2}$$

by incorporating a coefficient $\gamma(z)$ which reflects both the substrate-adsorbate and the adsorbate-adsorbate interactions, however Cheng and Cole showed that Eq. (2) can be well approximated by the form of the thin-film regime ($z \ll 5$ nm),[12,13]

$$k_BT\ln(p/p_0)=-\gamma_0 z^{-s}, \tag{3}$$

where γ_0 is a constant. The original DLP theory also fixed the exponent s to 3.

More recently, a fractal model based on the FHH theory was suggested for thick-film adsorption on a rough surface.[14] The analysis predicted the number of adsorbed molecules N as

$$N\propto[\ln(p_0/p)]^{(D/3-1)}, \tag{4}$$

where D is the fractal dimension of the surface. D has values from 2 to 3. In the case of a nonfractal surface, $D=2$ and Eq. (4) is reduced to the FHH equation with the exponent $s=3$. The rough Ag surfaces have a fractal dimension $D=2.30$.[14]

III. EXPERIMENT

We used an At-cut quartz resonator (radius $r_q=4.4$ mm) which was produced commercially. Originally the resonator was coated with Ag electrodes and had a fundamental resonance frequency $f_0=3.5798$ MHz. We further coated the resonator with a thin layer (thickness $d=2.9\times10^3$ Å) of porous silica (xerogel) following the standard alcoxide method using tetramethoxysilane (TMOS). The chemical reaction which occurred was

$$\mathrm{Si(OCH_3)_4+2H_2O\rightarrow SiO_2+4CH_3OH}. \tag{5}$$

To speed up the process, 0.069 mol % NH_4OH aqueous solution was added as a catalyst. A small quantity of the liquid mixture (NH_4OH solution 0.73 ml + methanol 1.8 ml + TMOS 3 ml) was dropped and spread onto both surfaces of the quartz resonator. It was then kept sealed at room temperature and allowed the gelation process to take place on the surfaces of the quartz crystal. The concentrations of the reactants were the same as for the production of bulk aerogels with 90% porosity when measured after hypercritical drying.

The thin layer gel was dried in air atmosphere and then in vacuum. *In situ* monitoring of the gelation and drying process was performed by measuring the resonance frequency f and amplitude of oscillation A of the quartz resonator. The resonance frequency decreased continuously while the amplitude increased with a large amount of random and abrupt fluctuations. The inverse amplitude $(1/A)$ is proportional to the acoustic impedance of the viscous layer in contact with the QCM. The decrease of the impedance results in the decrease of energy dissipation at the interfacial boundaries. It corresponds to the fact that the silica structure becomes harder as gelation proceeds and less liquid remains in the pores as the gel is dried. As time went on, the fluctuations in the amplitude of oscillations decreased. We evacuated the resonator for about a month before the isothermal adsorption measurements were performed. By that time, the frequency of the oscillation had dropped by about $\delta f \simeq -3.3$ kHz from the original resonance frequency f_0 of the resonator.

For a sample cell, we made a brass can with dimensions ϕ 30 mm and L 55 mm. The sample cell contained the quartz crystal resonator coated with a porous silica layer and a calibrated platinum resistance thermometer (Lakeshore, Pt100). The adsorbate (N_2 gas) was introduced into the sample cell through a stainless-steel tube (ϕ 6.4 mm). Temperature control of the sample cell was furnished by a heating wire coiled around the cell and a temperature controller (Lakeshore, DRC-91CA) with 0.01 K resolution. The sample cell was placed inside a continuous gas flow cryostat (Oxford, CF 1200) and liquid nitrogen flow was used to cool the sample cell indirectly. The temperature of the cryostat was controlled by a separate temperature controller (Oxford, ITC4) with 0.1 K resolution and adjusted to 4 K lower temperature than the sample cell.

We used a home-built Colpitts oscillator circuit operating at room temperature. The output from the oscillator circuit was split into two lines. One was connected to a frequency counter (FLUKE 1953A), with frequency resolution 0.1 Hz, and the other to a full-wave diode circuit. The oscillation amplitude was measured by a voltmeter (Keithly 182). The gas pressure of the sample cell was measured by a capacitance manometer (MKS 146) with 1 mTorr resolution. It took about 10 h to obtain an adsorption isotherm of N_2 in the pressure range $0 \leqslant p/p_0 \leqslant 1$. It was necessary to wait a long time to reach equilibrium near the saturation vapor pressure $(p/p_0 \simeq 1)$, due to the heat given off by the vapor condensing in the pores.

IV. RESULTS AND DISCUSSION

A planar surface of the AT-cut quartz crystal which is driven by a periodic driving force $F(\omega)=F_0 e^{i\omega t}$ with angular frequency ω will oscillate in a direction parallel to the plane with a velocity $v(\omega)=v_0 e^{i\omega t}$. The ratio $Z = F_0/(v_0 S)$ is called the acoustic impedance, where S is the surface area of the plane.[15] The acoustic impedance is further expressed as $Z(\omega)=R(\omega)-iX(\omega)$. When the plane is in contact with the vapor, the real part $R(\omega)$ is given by $R(\omega)=\sqrt{\eta\rho\omega/2}$, where η and ρ are the viscosity and density of the vapor, respectively.[16] The amplitude of oscillation changes as $\delta(1/A) \propto R$. The imaginary part $X(\omega)$ is associated with the inertia of the oscillator and determines the resonance frequency shift. Gas molecules in contact with the quartz crystal surfaces cause a drop in the frequency of oscillation of the quartz due to viscous loading,[16]

$$-\delta f_{\text{viscous}} = \frac{2 f_0 \sqrt{\eta\rho\omega/2}}{\pi R_q}, \tag{6}$$

where f_0 is the resonance frequency, $\omega = 2\pi f$, and $R_q = 8.862 \times 10^6$ kg/m^2 s is the transverse acoustic impedance of quartz. Figure 1(a) shows the frequency shifts $-\delta f$ of the

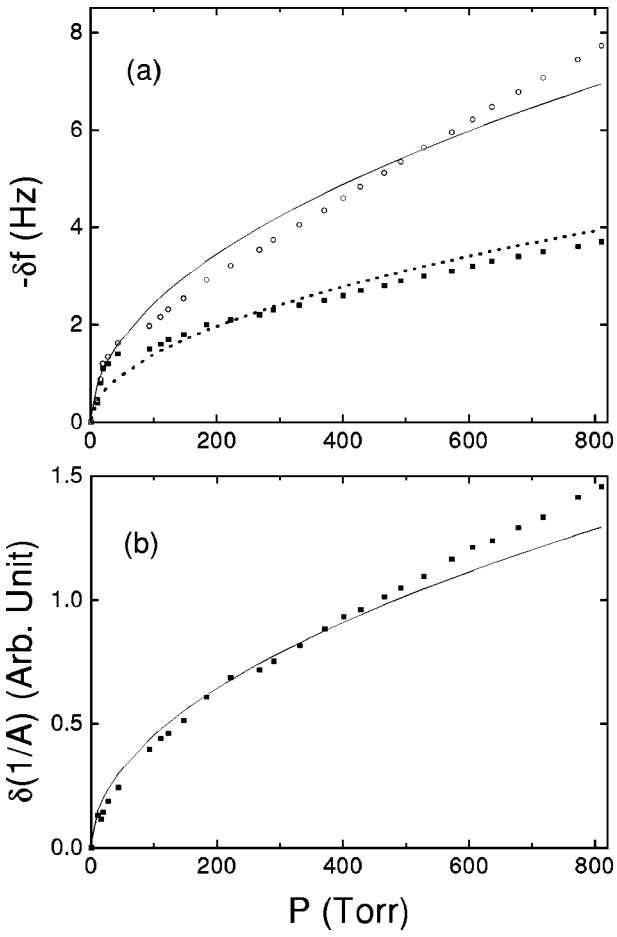

FIG. 1. (a) The frequency shifts (■) and (b) the changes in the inverse amplitude of oscillation of the QCM covered with a porous silica layer versus the pressure of N_2 gas at 325 K. Since no N_2 adsorption is expected at such a high temperature, we attribute the frequency shifts to the viscous loading effect. A dotted line is drawn for the expected frequency shift due to the viscous loading effect calculated from Eq. (6). The experimental data of frequency shifts after correction for the hydrostatic pressure effect (○) are about 1.8 times larger than those expected from the viscous loading of flat surfaces. A fitted curve is drawn for the enhanced viscous loading effect.

QCM coated with porous silica measured in N_2 gas atmosphere at 325 K. The dotted line in Fig. 1(a) indicates the expected frequency shifts due to the viscous loading effects [Eq. (6)] for a flat surface. We used an ideal gas law and $\eta \simeq 1.88\times10^{-5}$ kg m^{-1} s^{-1} for N_2 at 325 K.[17] The experimental data (filled squares) $-\delta f$ appear to be in good agreement with the calculated $-\delta f_{\text{viscous}}$.

However, this agreement is accidental since the hydrostatic pressure effect should be considered, too. The hydrostatic pressure effect is the increase in oscillation frequency associated with the vapor pressure, which compresses the quartz crystal faces. The frequency increases in proportion to the pressure, and the proportionality constant depends on both the temperature and cutting angle of the quartz crystal, but not on the kind of gases used. The empirical coefficient of the hydrostatic pressure effect is $(1/f)df/dp \simeq 13.6\times10^{10}$ torr^{-1} at 325 K for AT-cut quartz resonators.[16] The data corrected for the hydrostatic pressure effect (open circles) have additional frequency down shifts over those expected from the viscous loading effect. These additional frequency shifts cannot be explained by the mass loading effect, which is another mechanism of the oscillation frequency shifts, since no significant adsorption of N_2 is expected at such a high temperature (i.e., $T=325$ K). An explanation for the extra frequency shifts can be found from the porous structure of the substrate coated on the quartz resonator. Since the porous silica substrate is rough and has a large internal surface area, it can increase the viscous loading of the QCM. In our case the acoustic impedance $R(\omega)$ has been increased by a factor of 1.8 as indicated by the curved line in Fig. 1(a).

Figure 1(b) shows the changes in the inverse amplitude of oscillation $\delta(1/A)$ as a function of N_2 vapor pressure. The line in Fig. 1(b) shows data fitted using the relation $\delta(1/A) \propto \sqrt{p}$. Deviation of the data from the fit line in the region $p > 400$ torr indicates that there exists excessive energy dissipation over the viscous loading of flat surface. The deviation increases with p and is possibly related to the porous structure of the silica layer. With respect to the enhanced viscous loading exerted by the adsorbates, Watts *et al.*[15] reported an experimental observation of interfacial slippage of the adsorbed liquid film. This was evidenced by the fact that the measured acoustic impedance was larger than that expected theoretically. Since the slippage of the adsorbed liquid layer increased the acoustic impedance, the oscillation amplitude was, as a result, decreased. This phenomenon has been utilized to probe sliding-friction effects by Krim *et al.*[18]

Figure 2 shows the frequency shifts $-\delta f$ versus the pressure of N_2 for the porous silica substrate during adsorption (filled squares) and desorption (open circles) processes at 77.9 K. These data have been corrected for the hydrostatic pressure and viscous loading effects in the same way as high-temperature analysis. (We used $\eta \simeq 5.37\times10^{-6}$ kg m^{-1} s^{-1} for N_2 (Ref. 15) and $(1/f)df/dp \simeq 16.0\times10^{10}$ torr^{-1} at 77.4 K.[16]) Although there remains an ambiguity in the correction as shown in the high-temperature data, the correction is less than 4 Hz at most and negligible for the low-temperature measurements. Frequency shifts at 77.9 K are more than 10 times larger than at 325 K. An eminent hysteresis appears in the adsorption and desorption isotherms in the region $0.65 \leqslant p/p_0 \leqslant 1$. The hysteresis is an indication of the

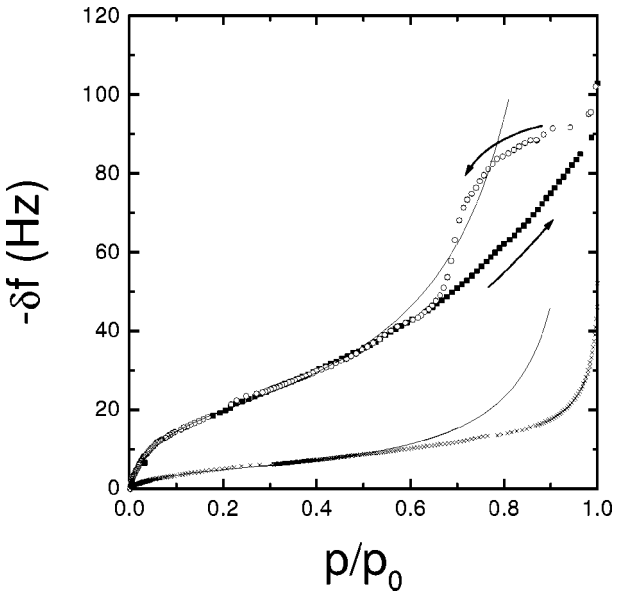

FIG. 2. The frequency shifts versus the normalized pressure of N_2 at 77.9 K. The frequency shifts for the quartz crystals were measured during the adsorption (■) and desorption (○) processes on the porous silica substrate. At low temperature, the mass loading effect dominates the frequency shifts. There is hysteresis (arrows) between the adsorption and desorption curves. The frequency shifts for a quartz crystal with Ag electrodes (×) were measured for the same conditions and are shown together. BET curves are drawn to fit the data.

capillary condensation and results from the mesoscopic size [10–250 Å (Ref. 9)] pores or capillaries in the porous silica substrate. The isotherms are of the so-called type IV according to Brunauer's classification.[9] In order to compare with the adsorption on a flat substrate, the frequency shift was measured using a QCM without a porous silica substrate, too. The data after correcting for the hydrostatic pressure and viscous loading effects are shown together in Fig. 2 and indicate fewer frequency shifts. Furthermore, there is no hysteresis observed from the flat substrate.

A thin film adsorbed uniformly onto the quartz crystal surface causes a drop in oscillation frequency,

$$-\delta f_{\text{mass}} = \frac{4f_0^2}{R_q}\frac{\Delta m}{S}, \tag{7}$$

where Δm is the mass of the film adsorbed and S is the area of the surface.[16] Equation (7) is valid for weak loading, i.e., $\Delta m \ll M_q$, where M_q is the mass of the quartz crystal.

Generally, the Brunauer-Emmett-Teller (BET) analysis[9] is used to determine the surface area from the adsorption isotherm. The BET analysis is applicable to the adsorption of gases up to a few layers. In the BET model, the adsorption of molecules on a surface is considered as an activated process. The BET equation can be expressed as

$$\frac{p/p_0}{n(1-p/p_0)} = \frac{1}{n_m c} + \frac{c-1}{n_m c}(p/p_0), \tag{8}$$

where n is the number of adsorbed molecules, n_m the number of molecules required to complete a monolayer, and c is $\exp(-(E_{\text{ads}}+E_L)/k_BT)$. Here E_{ads} corresponds to the activa-

tion energy for the first-layer adsorption and E_L is the latent heat. For further adsorption beyond the first layer, the activation energies are assumed to be equal to E_L. Equation (8) fits our data well for the adsorption up to a few layers ($0 \leqslant p/p_0 \leqslant 0.4$), as shown in Fig. 2.

From Eq. (7) we can infer that the 1 Hz decrease in frequency corresponds to adsorption of 2.3×10^{14} molecules. From the desorption data in Fig. 2, we obtain $n_m \simeq (4.4 \pm 0.1)\times10^{15}$. Using the specific surface area 3.54^2 Å^2 of the adsorbed N_2,[9] the surface area of the porous substrate is found $S = 5.5 \pm 0.1$ cm^2. This is nine times larger than the apparent area of the quartz crystal, which is about 0.6 cm^2. On the other hand, the calculated surface area using the data in Fig. 2 for the quartz crystal without a porous silica layer amounts to 1.35 ± 0.02 cm^2. This is about twice as large as the apparent area of the crystal. We attribute the difference to the roughness of the Ag electrode as well as the quartz crystal surface.

Using the frequency drop $\delta f_0 \simeq -3.3$ kHz, due to the porous silica layer, the mass of the porous silica layer is found $\Delta m \simeq 3.5\times10^{-5}$ g and this corresponds to the thickness of the layer 2.9×10^3 Å. Then, the estimated specific surface area of the porous silica is 18.5 m^2/g. Although this value is smaller than that of a typical xerogel ($\sim 10^2$ m^2/g[19]), the silica layer indeed has many pores and capillaries.

From the hysteresis in the adsorption and desorption curves, one may expect that the frequency decrease by 93 Hz corresponds to complete filling of the pores with 2.1×10^{16} N_2. Then the porosity of the silica layer is found to be $\sim$7.5% using the specific gravities of liquid N_2 ($\rho_{sg} = 0.81$) and of the silica layer ($\rho_{sg} = 2.3$).[17] In order to make a xerogel with large porosity, complicated procedures such as surface modification and aging are required.[19,20] In this experiment, however, we skipped the procedures and a large amount of shrinkage of the gel is expected. The volume of xerogel can be reduced by a factor of 5 to 10 compared to the wet gel.[19] We attribute the low porosity of xerogel to the shrinkage. As the N_2 gas pressure approaches the saturation vapor pressure ($p/p_0 \rightarrow 1$), condensation of the adsorbate is expected. However, a sharp increase in the frequency shift, which is a signature of condensation, was not seen in our experiment. Instead, the frequency shift increased steadily for a wide range of pressures $p/p_0 > 0.4$. The small-size pores result in less saturation vapor pressure than the bulk value p_0.[8,9] From the smooth increase and decrease of the adsorption and desorption curves, respectively, it can be expected that the pore sizes are distributed in a broad range.

We prepared a second QCM following the same steps. From the BET analysis on the second QCM, the surface area of the porous silica substrate was found $S = 3.7 \pm 0.1$ cm^2, corresponding to a thinner layer. Figure 3 shows the adsorption isotherms measured at three different temperatures above the bulk triple point ($T_t = 63.15$ K) of N_2: 76 K (filled squares), 77 K (open squares), and 80 K ($\times$), respectively. Although the bulk saturation vapor pressure p_0 is different at each temperature, all the adsorption curves merge onto a single curve after normalizing the pressures against the relevant saturation vapor pressure p_0. [See Fig. 3(a).] Recently, there appeared a Brief Report about the temperature-dependent adsorption of N_2 on porous vycor glass.[21] The

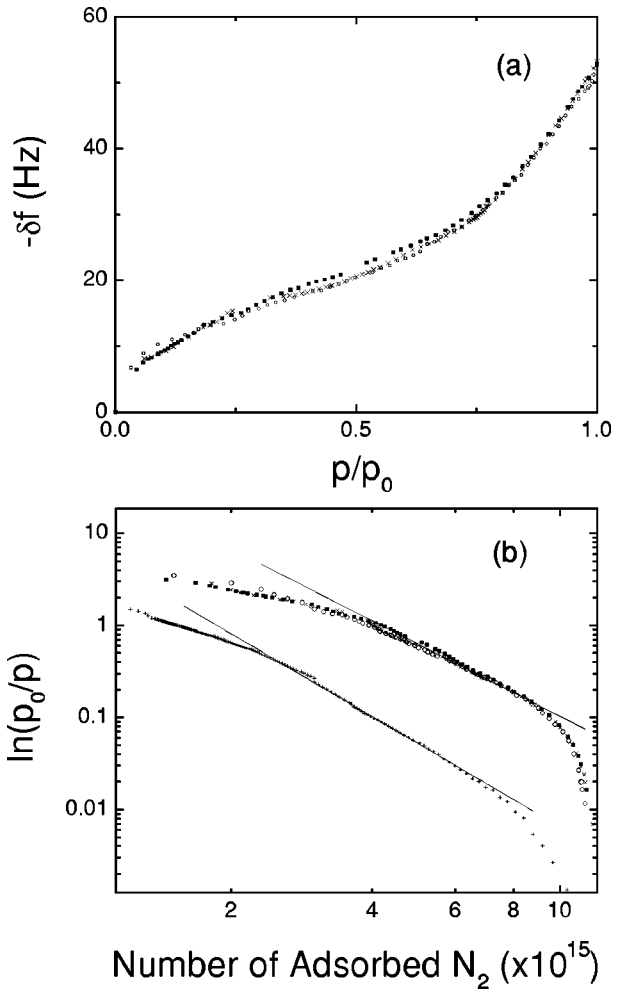

FIG. 3. (a) The frequency shifts versus p/p_0 at 76 (■), 77 (○), and 80 K ($\times$). (b) The same experimental results in (a) were replotted according to the DLP analysis, from which a straight line in the log-log plot is expected. The data are fitted with $-\delta f \propto N \propto [\ln(p_0/p)]^{1/s}$ and the slope given in the figure corresponds to $s \simeq 2.6 \pm 0.1$. For comparison, the frequency shifts of an Ag-electrode quartz crystal without the porous silica layer (+) are shown together. The straight line in this case corresponds to $s \simeq 3.0 \pm 0.1$.

adsorption isotherms at different temperatures were claimed to have different values of n_m and c, in a temperature range between 77 K and 120 K. However, we cannot see any evidence of a temperature dependence of n_m or c from our study.

The isotherms were replotted as $\ln(p_0/p)$ versus the number of adsorbed molecules in a log-log plot [Fig. 3(b)], where the number was calculated from the frequency shift measurements using the BET equation [Eq. (8)]. The exponent s and coefficient γ_0 in the modified Eq. (3) can be determined from this plot. However, not all the data lie on a straight line in Fig. 3(b) and there is ambiguity in determining which is the power-law region. Since the FHH and DLP theories are mostly applicable to multilayer adsorption regions and the porous silica has incomplete condensation, we select the region in between the monolayer adsorption and condensing regions to fit to the theory. The results are $s = 2.6 \pm 0.1$ and $\gamma_0 \simeq 5040 \pm 100$ K Å^3. A value of exactly 3 is expected for the exponent s according to the FHH and DLP theories. The data of the quartz crystal without a porous silica layer

(crosses) indeed show $s=3.0\pm0.1$ and $\gamma_0\simeq18\,000\pm1000$ K Å^3, which is in good agreement with the results of N_2 adsorption on Au.[12] There are examples suggesting the exponent s should be smaller than 3. With N_2 at 77 K, $s\simeq2.75$ for hydroxylated silicas was reported, with even lower values (2.2–2.48) for dehydroxylated silicas.[9] Furthermore, Drake *et al.*[22] claimed that their analysis for N_2 adsorption on silicagel was model-dependent and could not provide any clear-cut information on the morphological features of the surface. On the other hand, the values of s, according to Halsey,[10] can be taken as a rough estimate of the strength of interactions between the adsorbate and substrate. As a result, our experimental value $s\simeq2.6$ is in good agreement with other experimental results and may not be considered as an indication of the fractal nature of the adsorption on the porous silica substrate.

The measured γ_0 is larger than that expected for the silica substrate from the FHH or DLP theory, 3590 or 4630 K Å^3, respectively.[12] From our results it is noticeable that γ_0/k_BT is temperature-independent in the temperature range between 76 K and 80 K and the number of molecules adsorbed is temperature-independent, too. Recently, Sukhatme *et al.*[23] studied wetting of Ar on gold near the triple point of Ar ($T_t=83.31$ K). According to the thermodynamic model they studied for the triple point wetting, the free energy for liquid Ω_l at $T>T_t$, lies below both Ω_s for solid and Ω_{layer} for liquid/solid layered films and does not depend on temperature. It is well known that N_2 adsorption shows the triple point wetting.[2] The temperature-independent adsorption data we obtained at $T>T_t$ are consistent with Sukhatme *et al.*[23]

In the condensing region where $p/p_0\rightarrow1$, the adsorption does not proceed strongly and the adsorption isotherms deviate from the straight line in Fig. 3(b). Mecke *et al.*[24] suggested that deviations in the intermediate adsorption region are due to thermal fluctuations. The thickness of the adsorbed layer fluctuates at a given temperature, which results in a kind of surface tension. Contrary to our results, however, thermal fluctuations increase the adsorption in the intermediate region. We attribute the deviation to the porous structure. Considering that the FHH and DLP theories are suitable for a flat substrate, it may be absurd to apply those theories to the condensing region of porous substrates. As $p\rightarrow p_0$, the adsorbed layer thickens up to mesoscopic scale. Then, the small pores will be filled with the adsorbed liquid, whereas the large pores are partially filled and the substrates have reduced surface areas and pore volumes. Generally, this effect is utilized to measure the pore size distribution of porous media.[9] The effectively reduced surface area decreases the adsorption and makes the adsorption curves deviate from the power-law relation. This deviation is thus another indication of the porous structure of the silica substrates.

V. CONCLUSION

When a quartz crystal resonator coated with a thin porous silica layer was oscillated within a nonadsorbing vapor environment, the acoustic impedance related to the viscous loading increased due to the porous structure. We found a power-law relation between $k_BT\ln(p/p_0)$ and the amount of N_2 adsorbed on the rough silica in the intermediate coverage region. The exponent s and the coefficient γ_0 of the power-law relation in the temperature range 76 K–80 K were temperature independent with $s\simeq2.6\pm0.1$ and $\gamma_0\simeq5040\pm100$ K Å^3, which does not agree with DLP or FHH.

ACKNOWLEDGMENTS

This work was supported partially by the Ministry of Education, Korea through the Basic Science Research Institute, Seoul National University and by the Korea Science and Engineering Foundation through the Science Research Center for Dielectric and Advanced Matter Physics.

[1] David A. Huse, Phys. Rev. B **29**, 6985 (1984).
[2] J. Krim, J. G. Dash, and J. Suzanne, Phys. Rev. Lett. **52**, 640 (1984).
[3] G. B. Hess, M. J. Sabatini, and M. H. W. Chan, Phys. Rev. Lett. **78**, 1739 (1997).
[4] J. W. Cahn, J. Chem. Phys. **66**, 3667 (1977).
[5] E. Cheng, G. Mistura, H. C. Lee, M. H. W. Chan, M. W. Cole, C. Carraro, W. F. Saam, and F. Toigo, Phys. Rev. Lett. **70**, 1854 (1993).
[6] C. Carraro and M. W. Cole, J. Low Temp. Phys. **89**, 597 (1992).
[7] S. Brunauer, P. H. Emmett, and E. Teller, J. Am. Chem. Soc. **60**, 309 (1938).
[8] W. A. Steele, *The Interaction of Gases with Solid Surfaces* (Pergamon, Oxford, 1974).
[9] S. J. Gregg and K. S. W. Sing, *Adsorption, Surface Area and Porosity* (Academic Press, London, 1982).
[10] G. D. Halsay, J. Chem. Phys. **16**, 931 (1948).
[11] I. E. Dzyaloshinskii, E. M. Lifshitz, and L. P. Pitaevskii, Adv. Phys. **10**, 165 (1961).
[12] E. Cheng and M. W. Cole, Phys. Rev. B **38**, 987 (1988).
[13] V. Panella, R. Chiarello, and J. Krim, Phys. Rev. Lett. **76**, 3606 (1996).
[14] P. Pfeifer, Y. J. Wu, M. W. Cole, and J. Krim, Phys. Rev. Lett. **62**, 1997 (1989).
[15] E. T. Watts, J. Krim, and A. Widom, Phys. Rev. B **41**, 3466 (1990).
[16] C. D. Stockbidge, *Vacuum Microbalance Techniques* (Plenum, New York, 1966), Vol. 5.
[17] *CRC Handbook of Chemistry and Physics*, 60th ed., edited by R. C. Weast (CRC Press Inc., Boca Raton, FL, 1979).
[18] J. Krim, D. H. Solina, and R. Chiarello, Phys. Rev. Lett. **66**, 181 (1991).
[19] C. J. Brinker and G. W. Scherer, *Sol-Gel Science, The Physics and Chemistry of Sol-Gel Processing* (Academic, San Diego, 1990).
[20] S. V. Nitta, V. Pisupatti, A. Jain, P. C. Wayner, Jr., W. N. Gill, and J. L. Plawsky, J. Vac. Sci. Technol. B **17**, 205 (1999).
[21] T. E. Huber and H. L. Tsou, Phys. Rev. B **57**, 4991 (1998).
[22] J. M. Drake, L. N. Yacullo, P. Levitz, and J. Klafter, J. Phys. Chem. **98**, 380 (1994).
[23] K. G. Sukhatme, J. E. Rutledge, and P. Taborek, Phys. Rev. Lett. **80**, 129 (1998).
[24] K. R. Mecke and J. Krim, Phys. Rev. B **53**, 2073 (1996).